Proceedings 10th NUMGE 2023
10th European Conference on Numerical Methods in Geotechnical Engineering
Zdravkovic L, Kontoe S, Taborda DMG, Tsiampousi A (eds)

https://doi.org/10.53243/NUMGE2023-142

Calibration of cyclic soil degradation models through the discrete element method

F. Maksimov [1], A. Tombari [1]

[1]*School of Architecture, Technology and Engineering, University of Brighton, Brighton, UK*

ABSTRACT: Cyclic soil degradation models are used to capture the undrained behaviour of soils subjected to cyclic loading. Under these conditions, a progressive variation of the soil strength can occur, eventually leading to soil liquefaction. These models require relationships between the degradation of the soil properties and the number of loading cycles which can be derived from controlled laboratory tests. Unfortunately, a large number of tests would be required to account for every parameter affecting the cyclic soil behaviour. On the other hand, the Discrete Element Method (DEM) offers an interesting approach to simulate the complex behaviour of an assembly of particles. This study deals with the potential use of the DEM to simulate cyclic undrained triaxial testing with the aim to derive soil damage relationships. Different grain-size distribution curves of sands are tested at different confining pressures with different axial strain levels. The effect of particle-size distribution on the results is examined and compared with published experimental cyclic triaxial tests. Laws to describe the random effects of the number of loading cycles on the strength are proposed.

Keywords: DEM; Liquefaction; Sand; Soil Fatigue Models.

1 INTRODUCTION

Cyclic loads applied to sandy soils under undrained conditions can determine the degradation of their geotechnical properties, such as strength and stiffness. This phenomenon is particularly relevant in loose sands where the contractive tendency causes the porewater pressure build-up while decreasing the effective stresses on the soil skeleton at each cycle. Consistently, the partial or total loss of soil stiffness and strength is manifested, which can lead to an increment of the internal forces on the foundations (Tombari et al., 2017). This phenomenon can lead to soil liquefaction, which has been extensively studied over the last decades. Recently, an international collaborative research project denominated „*The Liquefaction Experiments and Analysis Projects (LEAP)*“ aimed to provide experimental data for the calibration and validation of constitutive models used by different researchers (Kutter et al., 2019). Results from physical testing were used by 11 different academic institutions and geotechnical engineering companies across the world for the calibration of continuum constitutive models. The results of the cyclic triaxial testing can be also used to determine empirical parameters characterizing soil fatigue models (see e.g., Allotey and El Naggar, 2007). Because of the various parameters affecting the soil response, e.g., confining pressure, void ratio, and particle size distribution, several tests are required for a reliable calibration of any constitutive soil model. Therefore, Maksimov and Tombari, (2022) exploited the discrete element method (DEM) to simulate the dilative/contractive behaviour of an assembly of particles which is a crucial aspect of the cyclic response. A series of numerical cyclic triaxial tests of uniform granular media were carried out to assess the deviatoric stress change at each cycle. This approach was used by Zorzi et al., (2017), to simulate the long-term cyclic drained behaviour of sands. In this paper, the experimental result of the LEAP exercise has been used to perform calibration and validation of the DEM model. The effect of the uncertainty of the particle-size distribution on the undrained cyclic response is examined through Monte Carlo Simulation. Numerical results are used to determine the parameters of the soil fatigue model developed by Allotey and El Naggar (2007) considering soil uncertainties.

2 NUMERICAL CYCLIC TRIAXIAL TESTING

2.1 Ottawa F-65 sand

The soil investigated in this paper is the Ottawa F-65 sand which was adopted as the standard testing soil in the collaborative LEAP project (ElGhoraiby et al., 2020). It is an inert, white silica sand of rounded grains with a quartz content of 99.7%. The Ottawa F-65 sand is classified as poorly graded sand (coefficient of uniformity, C_u=1.73) with a fines content of less than 0.5% fines. The average grain size distribution is given in Figure 1.

2.2 Discrete Element Method model

Amongst the methods to simulate the macroscopic mechanical behaviour of soils, the Discrete Element Method (DEM) is an appealing technique where individual grains are modelled by disk or spherical particles. Therefore, the advantage of the DEM is the ability to simulate directly and intrinsically the dilative or contractive behaviour of granular soils. Through an explicit integration scheme, contact forces are evaluated using the velocity and position of particles at every time step. In this study, the linear spring contact law (Cundall and Strack, 1979) with rolling stiffness was applied and is assumed for simulating particle-particle interactions. The open-source DEM software YADE (Kozicki and Donzé, 2008) is used to create and simulate the soil samples.

2.3 Numerical sampling preparation

The three-dimensional assembly of particles (around 3000) is created by randomly generating spheres of radius that are drawn from the particle size distribution (PSD) of Figure 1 which can be interpreted as a cumulative distribution function. The spheres' radii range from a minimum of 0.075 mm to a maximum of 0.85 mm. The particles are first enclosed in a cubic cell of 0.04m in size in order to avoid any initial contact, hence, creating a random gas-like cloud of particles.

A period boundary condition for modelling the cell boundaries (Kozicki et al., 2014) is used. The cloud of particles is then subjected to isotropic compression by moving uniformly the cell boundaries until the mean stress reaches the test confining pressure. Subsequently, the interparticle friction angle is reduced to decrease the void ratio by keeping a constant confining pressure; this procedure allows fixing the initial void ratio at a given confining pressure.

After this procedure, the parameter of the interparticle friction angle can be reassigned through the calibration procedure. The physical sample used as a reference in this paper is characterized by an initial void ratio of 0.608 subjected to a confining pressure of 100kPa and 200kPa, as in ElGhoraiby et al., (2020) and Vasko, (2015).

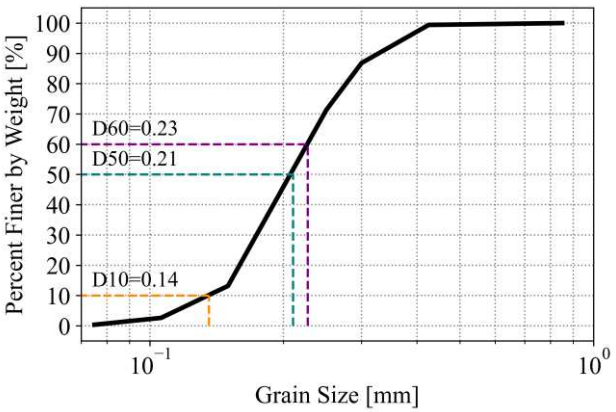

Figure 1. Ottawa F65 average grain size distribution

2.4 Strain-controlled cyclic triaxial testing

The second phase consists of strain-controlled cyclic triaxial testing. The assembly of particles is subjected to cyclic deviatoric stress induced by controlling the strain levels of the sample boundaries. Since the pore pressure is not modelled, the simulation of the undrained conditions is achieved through a constant volume approach obtained by constraining the strains in the three directions as follows (Martin et al. 2020; Maksimov and Tombari, 2022):

$$\varepsilon_{xx} = \varepsilon_{yy} = -0.5 \cdot \varepsilon_{zz} \quad (1)$$

in which ε_{xx} and ε_{yy} are the strains of the lateral boundaries of the periodic cell, whilst ε_{zz} is the axial strain aligned with the cyclic direction during the triaxial testing.

The cyclic loading is then imposed through the following relation:

$$\dot{\varepsilon} = \varepsilon_{zz}^{max} \cdot 2\pi f \cdot \cos(2\pi f t) \quad (2)$$

where f is the frequency (fixed at 0.0083 Hz as in Vasko, 2015), ε_{zz}^{max} is the maximum axial strain, t is the current time in seconds. A numerically stable simulation is achieved by setting the critical time step size equal to the minimum time needed for the elastic P-waves to travel across a particle as follows (Radjai and Dubois, 2011):

$$\Delta t_{min} = 2 \cdot \sqrt{\frac{m_i}{k_n}} \quad (3)$$

where m_i and k_n is the particle mass and normal stiffness.

Since the maximum strain rate is kept lower than the quasi-static threshold (Radjai and Dubois, 2011), the particle mass density is not affecting the stress-strain behavior, and hence can be set to a high value of 10^{12} kg/m^3 to reduce the computational cost (Thornton and Antony, 1998).

The simulation stops when the maximum deviatoric stress at the current cycle is reduced to 10% of the maximum deviatoric stress recorded at the first cycle.

In this paper, this criterion is used as the liquefaction onset value or maximum stress degradation value.

2.5 Calibration of the DEM parameters

The governing equations of the DEM model and contact law defined in Section 2.2 can be fully determined by 7 parameters which are assigned to each *ith*-particle: the radius, r_i and the mass density of each particle, m_i, the normal stiffness, k_n, the Poisson's ratio, υ, the interparticle angle of friction, φ, the rolling stiffness coefficient, α_r, and the limiting rolling coefficient, η.

In this paper, 3 parameters are considered for the calibration of the contact law: the interparticle friction, μ,

and rolling friction, η^r, both responsible for the model plastic behaviour (De Pue et al., 2019) and the normal stiffness parameter, k_n. The other parameters shown in Table 1 are derived from the particle size distribution or kept fixed to simplify the calibration analysis.

In the first instance, a heuristic approach is used; the method consists of two steps, first calibration of the parameters, k_n and μ, to obtain the maximum deviatoric stress and initial stiffness of the backbone curve through a monotonic analysis and then, cyclic triaxial testing to obtain the target number of cycles to liquefaction by changing the parameter η_r. These 2 steps are repeated to obtain the best approximation of the results of a series of reference tests; Figure 2 shows the comparison of the simulated and measured stress-strain hysteresis after calibration of the parameters as in Table 1.

The asymmetric stress-strain behaviour is not well captured by the DEM model showing the limitation of the contact laws adopted for this study, which used linear elastic contact relations under tension and compression. On the other hand, the maximum deviatoric is well captured as expected by the proposed heuristic procedure and an acceptable error in simulating the liquefaction onset is achieved; in Figure 3 is depicted with a red-coloured curve of the axial strain – number of cycles to liquefaction obtained from the experimental results of the LEAP project; the blue coloured curve is obtained from the DEM results after calibrating the parameters as in Table 1. Each marker in Figure 3 represents an independent DEM analysis.

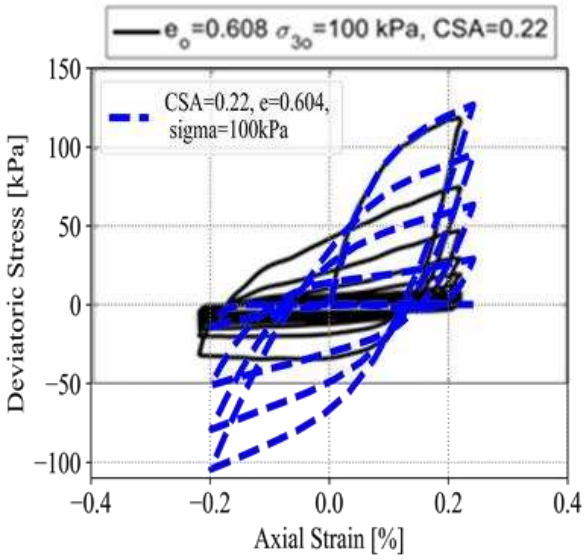

Figure 2. Stress-strain hysteretic behaviour (readapted from ElGhoraiby et al., 2020) – black curve: experimental results; blue - dashed curve: DEM simulation.

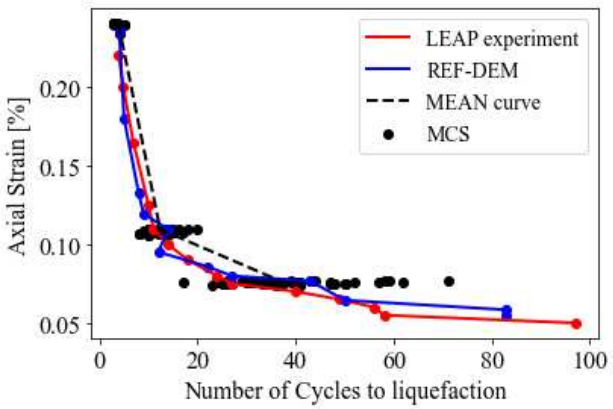

Figure 3. Calibration of the DEM model against the experimental $e_z - N_u$ curve (ElGhoraiby et al., 2020) and results of the Monte Carlo Simulation (MCS)

Table 1. DEM parameters after calibration

Parameter	Description	Value
k_n	normal stiffness N/m	$6.0E8$
ν	Poisson's ratio	0.2
α	rolling stiffness coefficient	2
μ	Frictional angle	17°
η_r	limiting rolling coefficient	0.15
r_i	ith-particle radius	variable
m_i	mass density $[kg/m^3]$	10^{12}

3 MONTE CARLO SIMULATION

The impact of the grain-size distribution on the cyclic soil degradation is investigated by performing a Monte Carlo simulation of numerical cyclic triaxial testing in which several samples of particle size distribution functions representing the Ottawa F-65 sand are considered. A total of 140 soil samples were tested in undrained conditions at a confining pressure of 100kPa for 3 levels of strain and 150 soil samples were subjected to the confining pressure of 200kPa for 5 levels of strain. Validation of the average results is also presented in this section.

3.1 Random granulometry

The particle size distribution (PSD) functions are randomly generated during the sampling preparation as explained in Section 2.3 by considering the PSD of the Ottawa F-65 sand of Figure 1 as the mean function; the mean passing percentage at each sieve is reported in Table 2. The dispersion of the generated PSD functions is shown in Figure 4 with grey curves, whilst the red dashed curve represents the computed mean; a small dispersion from the reference curve is obtained, as also determined by the coefficient of variation (COV) in Table 2.

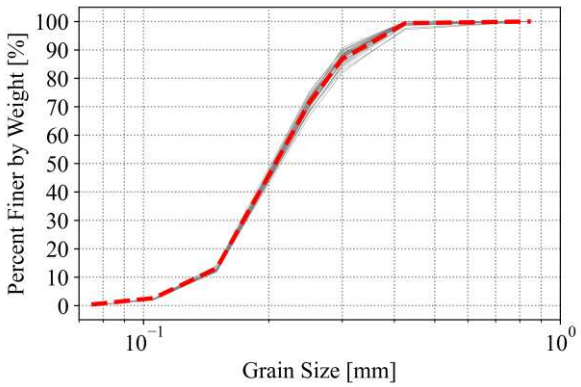

Figure 4. Generated PSD curves (grey colour) and mean PSD of the Ottawa F65 sand (dashed curve)

Table 2. Statistics of the generated particle size distribution functions

D [mm]	Mean passing [%]	COV
0.000075	0	0
0.000106	2.303	0.067
0.00015	12.937	0.050
0.00025	71.742	0.029
0.0003	87.089	0.023
0.000425	99.677	0.007
0.00085	100	0

Table 3. Statistics of the Number of Cycles to Liquefaction at the confining pressure of 100kPa

Max Axial Strain [%]	0.07	0.1	0.22
N_U^{mean}	37.27	12.36	3.83
N_U^{COV}	0.29	0.21	0.15
N_U^{exp}	40	14	3.9

Table 4. Statistics of the Number of Cycles to Liquefaction at the confining pressure of 200kPa

Max Axial Strain [%]	0.075	0.1	0.2	0.3	0.4
N_U^{mean}	30.77	13.23	4.23	2.67	2.27
N_U^{COV}	0.26	0.25	0.18	0.2	0.2
N_U^{exp}	16	7	6	5	3

After conducting cyclic triaxial testing at different confining pressure, axial strain on multiple samples, the statistics of the number of cycles to liquefaction are reported in Table 3 and Table 4 for the confining pressure of 100kPa and 200kPa, respectively. It can be observed that as expected, by increasing the maximum axial strain, the soil degradation occurs faster, i.e., with fewer cycles. Remarkably, although the dispersion of the PSD was small (COV < 7%), the propagation of the uncertainty is large, with COV greater than 15% and increasing with the decrease of the applied maximum axial strain. Results for the confining pressure of 100 kPa, are shown in Figure 5.

3.2 Validation of the DEM sand model

The calibrated DEM model is validated with the laboratory experiments carried out by Vasko (Vasko, 2015). Strain-controlled cyclic triaxial tests were conducted at the confining pressure of 200kPa to specimens of void ratio equal to 0.608, reported with a red curve in Figure 6. The results of the numerical simulation are reported for each of the generated samples with a dotted marker; the mean value shows a good correspondence with the reference experimental curve.

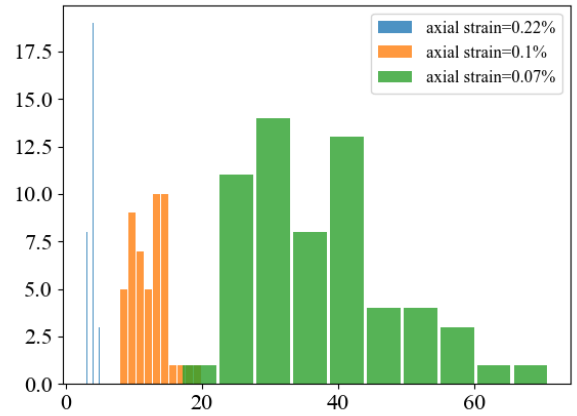

Figure 5. Distribution of the Number of Cycles to liquefaction for different axial strain levels at the confining pressure of 100 kPa

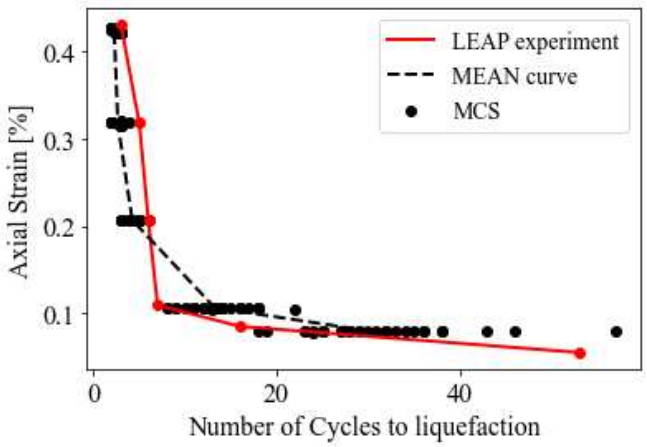

Figure 6. Verification of the DEM model against the experimental $e_z - N_u$ curve (Vasko, 2015) and results of the Monte Carlo Simulation (MCS)

4 DEGRADATION FATIGUE MODEL

The stress-independent elliptical function proposed by Allotey and El Naggar (2008) is considered for simulating the cyclic degradation of the Ottawas F-65 sand. The law is described by the following formula:

$$\delta_s = 1 + (\delta_f - 1)\left[1 - (1 - D)^{\theta}\right]^{\frac{1}{\theta}} \quad (4)$$

where δ_s is the strength degradation index, $\delta_f = 0.1$ is the liquefaction onset limit, θ is an empirical curve shape parameter and D is the damage factor. The strength degradation index δ_s is obtained as the ratio between the maximum deviatoric stress at the current cycle, N_c, and the maximum deviatoric stress obtained from a monotonic triaxial test.

In this paper, the damage factor is expressed as follows:

$$D = \frac{N_c}{N_U} \tag{5}$$

i.e., the ratio between the current cycle, N_c, and the cycle, N_U, corresponding to the liquefaction onset, δ_f. In the beginning, $D = 0$ and $\delta_s = 1$, while at N_f, $\delta_s = \delta_f$. The model requires the definition of two functions: the Wöhler curves, here represented as $\varepsilon_{zz}^{max} - N_U$ curve for strain-controlled testing, and the degradation curve expressing the relation between δ_s and the N_c, which is fully defined when the empirical curve shape, parameter, θ, is defined.

The latter is normally obtained through regression analysis as done in Allotey and El Naggar (2008) using De Alba et al. (1976) experimental results; the computed θ is found to be ranged between $\theta = 0.7 - 1.1$. Therefore, in this study, results from the MCS of the DEM samples are analyzed;

Figures 7(a) and (b) show the variation of the mean strength degradation index with the increase of the number of cycles for confining pressure of 100kPa and 200kPa, respectively. The curvature of the curve changes with the increase of the number of cycles to liquefaction; for low values, a linear curve ($\theta = 1.0$) can be adequately fitted the results whilst a concave function ($\theta < 1.0$), is required for high number of cycles. Statistics of the fitted curve shape parameter θ are reported in Table 5 and 6. Figure 8 shows the Strength Degradation Index curves for ε_{zz}^{max}=0.075% at the confining pressure of 200kPa; the grey curves are obtained from the DEM simulations whilst the black-dashed curves are the degradation curves defined by Equation (4) where the curve shape parameter θ is fitted for each individual curve.

To fully characterize Equation (4), the relation $\varepsilon_{zz}^{max} - N_U$ should be also provided. Figures 3 and 6 report the MCS results and their mean values for the confining pressure of 100 kPa and 200 kPa, respectively. Statistics are reported in Tables 3 and 4. To examine the effect of the grain size distribution on the number of cycles to liquefaction, three regression models are considered. The first one considers the relationship with the macro parameter of the maximum axial strain, ε_{zz}^{max}, the second is a two-parameter regression model which entails 2 variables, ε_{zz}^{max} and either the coarse content (CC) defined as the percentage of particle diameter larger than 0.2 mm or D80, defined as the sieve diameter for which 80% of the grains are smaller than this value; the third is a three-parameter regression model considering all these variables.

Table 5. Statistics of the curve shape parameter θ for the cyclic tests at the confining pressure of 100kPa

Max Axial Strain [%]	**0.07**	**0.1**	**0.22**
θ^{mean}	0.69	0.83	0.9
θ^{COV}	0.06	0.04	0.05

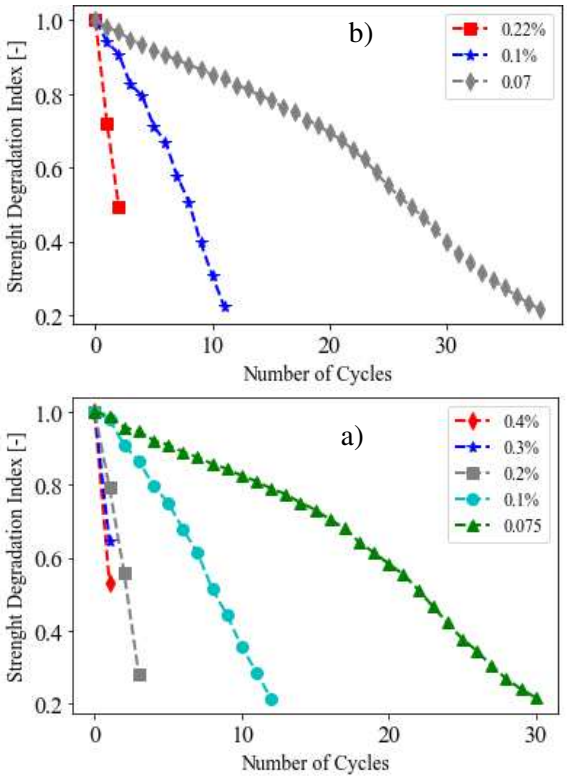

Figure 7. Average Strength Degradation Index curve for different ε_{zz}^{max} and confining pressure

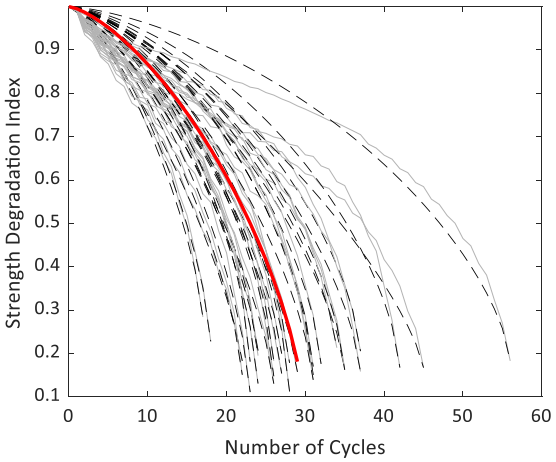

Figure 8. Strength Degradation Index curves for for $\varepsilon_{zz}^{max} = 0.075\%$ at the confining pressure of 200kPa; grey curves: DEM results; dashed curves: degradation law Eq. (4); thick curve: mean value.

Table 6. Statistics of the curve shape parameter θ for the cyclic tests at the confining pressure of 200kPa

Max Axial Strain [%]	**0.075**	**0.1**	**0.2**	**0.3**	**0.4**
θ^{mean}	0.72	0.80	0.93	0.84	0.75
θ^{COV}	0.05	0.04	0.03	0.13	0.12

The general regression model is defined as follows:

$$\ln(N_u) = a \cdot \ln(\varepsilon_{zz}^{max}) + b \cdot CC + c \cdot D80 + d \qquad (6)$$

where a, b, c, d are the regression coefficients obtained by fitting the results of the MCS carried out previously. Values are reported in Table 7. It is worth noting that the coefficient of determination, R^2, shows the strong correlation between the number of cycles to liquefaction, strain level and the parameter D80.

5 CONCLUSIONS

In this paper, numerical cyclic triaxial testing of sand samples has been carried out by using the Discrete Element Method (DEM). The typical grain size distribution of the Ottawa F-65 sand has been modelled, and a frictional contact law was used to simulate the normal, tangential and rolling behaviour. The cyclic behaviour of several soil samples was validated with experimental results conducted for the LEAP project. A Monte Carlo Simulation has been performed by generating about 300 soil samples and performing cyclic triaxial undrained testing at different confining pressures and levels of axial strain. Statistical regression analysis has been then performed to calibrate the soil damage model of Allotey and El Naggar (2008); results showed that the obtained parameters are consistent with the values indicated in the literature. The computed statistical quantities can be used to extend the deterministic soil damage model to random parameters for MCS of macro-models implementing this soil damage model.

Table 7. Coefficients of regression (for 100 and 200 kPa)

Model	**a**	**b**	**c**	**d**	**R^2**
ε_{zz}^{max}	-1.95	/	/	-1.57	0.89
	-1.54	/	/	-0.75	0.92
$\varepsilon_{zz}^{max} - CC$	-1.95	-0.05	/	1.56	0.9
	-1.54	-0.04	/	1.36	0.92
ε_{zz}^{max}	-1.97	/	-23.61	4.9	0.92
$- D80$	-1.53	/	-22	5.34	0.94
$\varepsilon_{zz}^{max} - CC$	-1.98	0.03	-29.23	4.59	0.92
$- D80$	-1.52	0.04	29.24	5.02	0.94

6 ACKNOWLEDGEMENTS

Dr Tombari gratefully acknowledges the financial support of the Engineering and Physical Sciences Research Council (EPSRC) through the New Investigator Award EP/W001071/1 “Structural Life-Cycle Enhancement of Next-Generation Onshore and Offshore Wind Farms”.

7 REFERENCES

Allotey, N., El Naggar, M. H. 2007. A consistent soil fatigue framework based on the number of equivalent cycles. *Geotechnical and Geological Engineering* **26**, 65–77.

Allotey, N., El Naggar, M.H. 2008. Generalized dynamic Winkler model for nonlinear soil–structure interaction analysis. *Canadian Geotechnical Journal* **45(4)**, 560-573.

Cundall, P.A., Strack, O.D. 1979. A discrete numerical model for granular assemblies *Geotechnique* ***29*****(1)**, 47-65.

De Alba, P.A., Chan, C.K., Seed, H.B. 1976. Sand liquefaction in large-scale simple shear tests. *Journal of the Geotechnical Engineering Division*, **102(9)**, 909-927.

De Pue, J., Di Emidio, G., Flores, R. D. V., Bezuijen, A., Cornelis, W. M. 2019. Calibration of DEM material parameters to simulate stress-strain behaviour of unsaturated soils during uniaxial compression, *Soil and Tillage Research* **194**, 104303.

ElGhoraiby, M. A., Park, H., Manzari, M. T. 2020. Stress-strain behavior and liquefaction strength characteristics of Ottawa F65 Sand, *Soil Dynamics and Earthquake Engineering* **138**, 106292.

Kozicki, J., Donzé, F. V. 2008. A new open-source software developed for numerical simulations using discrete modeling methods, *Computer Methods in Applied Mechanics and Engineering* **197(49-50)**, 4429–4443.

Kozicki, J., Tejchman, J., Mühlhaus, H. 2014. Discrete simulations of a triaxial compression test for sand by DEM. *Int. J. Numer. Anal. Methods Geomech*. **38**, 1923–1952.

Kutter B. L., Manzari M. T., Zeghal M. 2019. *Model tests and numerical simulations of liquefaction and lateral spreading: LEAP-UCD-2017*, Springer Nature.

Maksimov, F., Tombari, A. 2022. Derivation of cyclic stiffness and strength degradation curves of sands through discrete element modelling, *Modelling* **3(4)**, 400–416.

Martin, E. L., Thornton, C., Utili, S. 2020. Micromechanical investigation of liquefaction of granular media by cyclic 3D DEM tests, *Géotechnique*, **70(10)**, 906–915.

Radjai, F., Dubois, F. 2011. *Discrete-Element Modeling of Granular Materials*, Wiley-Iste, New York, NY, USA

Tombari, A., El Naggar, M. H., Dezi, F. 2017. Impact of ground motion duration and soil non-linearity on the seismic performance of single piles, *Soil Dynamics and Earthquake Engineering* **100**, 72–87.

Thornton, C., Antony, S. 1998 Quasi–static deformation of particulate media. *Philosophical Transactions of the Royal Society of London. Series A: Mathematical, Physical and Engineering Sciences* **356**, 2763-2782.

Vasko, A. 2015. *Liquefaction Resistance of Ottawa Sand F65*, M.Sc. Thesis, The George Washington University.

Zorzi, G., Kirsch, F., Gabrieli, F., Rackwitz, F., 2017. Long-Term Cyclic Triaxial Tests With Dem Simulations, in: Proceedings of the V International Conference on Particle-Based Methods - Fundamentals and Applications. Presented at the PARTICLES 2017, P. Wriggers, M. Bischoff, E. Oñate, D.R.J. Owen and T. Zohdi (Eds.), Hannover, Germany.